International Journal of Nanoelectronics and Materials
IJNeaM
ISSN 1985-5761 | E-ISSN 2232-1535

The Arc Current Effect on the Structure and Resistance of Nanoparticles

Miftahul Anwar[a,*], Riski Rama Kusuma[a], Teguh Endah Saraswati[b] and Feri Adriyanto[a]

[a]*Department of Electrical Engineering, Faculty of Engineering, Sebelas Maret University, Surakarta 57126, Central Java, Indonesia*
[b]*Department of Chemistry, Faculty of Mathematics and Natural Science, Sebelas Maret University, Surakarta 57126, Central Java, Indonesia*
**Corresponding author. e-mail: miftahwar@ft.uns.ac.id*

Received 17 July 2025, Revised 25 August 2025, Accepted 27 October 2025

ABSTRACT

This study investigates the influence of arc discharge current on the morphological, electrical, and plasma characteristics of carbon nanoparticles synthesized via submerged plasma arc discharge in deionized water. Arc currents of 40 A, 70 A, and 100 A were applied to graphite electrodes, and the resulting nanostructures were characterized using transmission electron microscopy (TEM), current-voltage (I–V) electrical measurements, and ionization energy analysis derived from time-resolved arc current behavior. The findings demonstrate that increasing the arc current significantly alters the morphology of the carbon products, transitioning from predominantly spherical carbon nano-onions (CNOs) at 40 A to multi-walled carbon nanotubes (MWCNTs) at 100 A. Concurrently, I–V characterization reveals an increasing trend in electrical resistance, rising from ~20 kΩ at 40 A to ~90 kΩ at 100 A, suggesting a strong correlation between nanostructure geometry and macroscopic conductivity. Ionization energy distributions derived from arc current dynamics further reveal a transition from continuous energy profiles at 40 A to highly discrete peaks at 100 A, indicating a shift in plasma species and energy transfer mechanisms. These discrete ionization profiles at higher currents are proposed to facilitate anisotropic carbon growth, favoring CNT formation through directed energy delivery and ion-assisted crystallization. This work elucidates the coupled roles of arc current, plasma behavior, and nanoparticle morphology in determining the structure and electrical properties of carbon nanomaterials synthesized via arc discharge.

Keywords: *Plasma arc-discharge, Carbon nanoparticles, Resistance, I-V measurement*

1. INTRODUCTION

Nanotechnology is a branch of science that studies material phenomena on a nanoscale [1]. It can also be interpreted as the science of applying technology to manipulate and manage problems at the nanoscale (1-100 nm), resulting in the size and structure of materials based on their properties [2]. In the last three decades, interest in carbon nanotechnology has increased rapidly. This is due to the development of accessible and cheap carbon synthesis methods [3].

Carbon is the fourth most abundant chemical element in the world. In addition to its abundance, carbon is also one of the most stable elements [4]. Carbon has the most allotropes compared to other materials, ranging from 0 to 3 dimensions [5]. Allotropes are chemically identical elements but very different in their physical properties. This occurs when carbon atoms form covalent bonds with other carbon atoms [6]. Some allotropes of carbon are included, such as graphene [7], buckminsterfullerene [8, 9], carbon nanotubes [10, 11], and many others.

Carbon nanotubes (CNTs) are allotropes of carbon with a nano-sized cylindrical structure [12]. CNTs continue to be attractive because they have small nanometer dimensions, large surface areas, very high mechanical strength, and low density [13], so they are very flexible, making CNTs a future smart material that has much potential to be applied in many fields [14]. In general, carbon nanotubes can be grouped based on the number of walls, namely, multi-walled carbon nanotubes (MWCNTs), single-walled carbon nanotubes (SWCNTs), carbon onions, and single-walled carbon nanohorns (SWCNHs) [15].

CNT synthesis can be done by several methods, including arc discharge [16], laser ablation, thermal synthesis process, chemical vapor deposition (CVD), vapor-phase growth, flame synthesis, plasma enhanced chemical vapor deposition (PECVD) [17]. In 1991, Iijima [11, 18] used arc discharge to produce MWNT CNTs after observing carbon soot produced from arc discharge using graphite electrodes with a current of 100 A.

In 2002, Sano [19] used a distilled water liquid medium instead of a vacuum chamber, later recognized as the submerged arc discharge method; this experiment produced carbon nano-onions. The advantages of the submerged arc discharge method are the relatively short process time, the use of simple equipment, and the production of products with relatively high purity [18, 20]. Our group conducted a submerged arc discharge experiment in 2018 [21] using pencil graphite as an electrode and distilled water as a liquid medium. Moreover, in 2022, we also developed current-voltage (I-V)-based spectroscopy for the arc discharge method for carbon nanoparticle synthesis using pure graphite as an electrode and tapering the negative electrode so that the electron

discharge was centered at one point while maintaining the current at 40A [22, 23].

This study aims to analyze the effect of different arc currents on the size, shape, and resistivity of produced nanoparticles. Submerge arc discharge experiments using distilled water as a liquid medium and varying currents (10A, 40A, 70A, 100A) produce nanoparticles with different sizes and different resistance values, so it is necessary to analyze the results of nanoparticles with this configuration. TEM is used to determine the structure of the nanoparticles produced, while Elkahfi 100/ I-V Meter is used to measure the resistance value of carbon nanoparticles.

2. EXPERIMENTAL SETUP

2.1. Submerged Arc Discharge

Graphite electrodes with 99.9% carbon purity in tubes with a diameter of 10 mm were used as anodes and cathodes, as shown in Figure 1. The anode and cathode were mounted horizontally on the welding clamp. The graphite positioned as the anode is tapered so that it is centered and accumulates more electrons in the tapered plane, while the graphite positioned as the cathode remains in the initial shape of the tube to have a larger area because when plasma occurs, electrons from the anode will jump to the cathode which will cause the cathode to decrease because it is eroded by the collision of electrons from the anode to the cathode. The electrode is connected to a DC arc welding inverter as a power source. The anode and cathode are immersed in a beaker containing distilled water in a plasma box.

The experiment was conducted four times with variations in the use of currents, i.e., 10A, 40A, 70A, and 100A. Then, the anode and cathode are moved closer to each other manually through the lever above the plasma box; when the distance between the anode and cathode is close enough for electrons to jump, the electrons will jump from the anode to the cathode. The transfer of electrons from the anode to the cathode will produce a spark called an arc that can be detected by a data analyzer [see Figure 1 (b)]. When the arc occurs, the cathode will be eroded, and the nanoparticles released from the cathode cause the liquid media to become cloudy and blackened over time. Separating nanoparticles from liquid media using the sedimentation method, using a centrifuge to separate nanoparticles from liquid media, and drying nanoparticles using a vacuum chamber to remove liquid media.

2.2. Carbon Nanoparticles Analysis Method

Transmission electron microscopy (TEM) and an Elkahfi 100/ I-V Meter were used to analyze carbon nanoparticle size distribution and resistance value, respectively. TEM analysis was conducted using HR TEM HITACHI H9500; 200kV. The TEM test results were obtained in the form of Bright Field Image (BFI). The nanoparticle size analysis data is obtained through manual BI measurements using ImageJ software by randomly measuring several nanoparticles, which are then presented as a nanoparticle distribution graph.

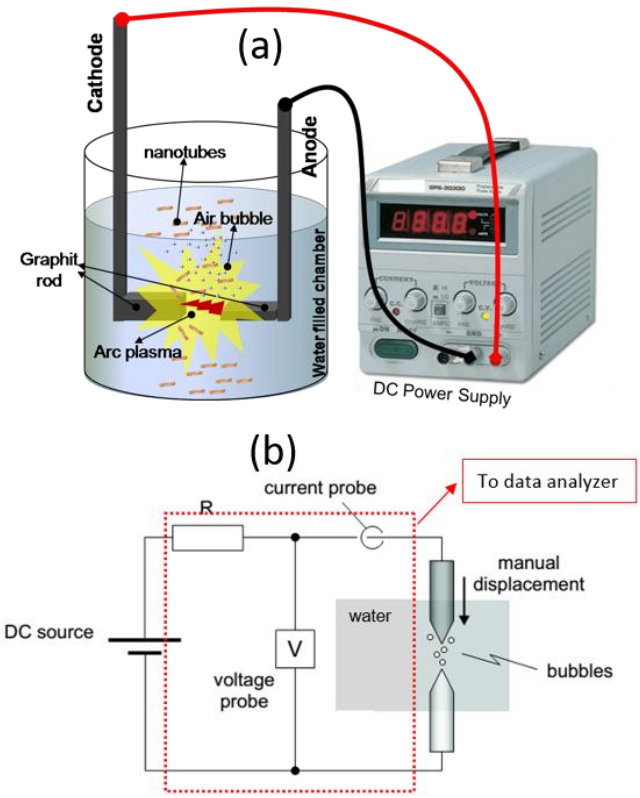

Figure 1. (a) Schematic illustration of the underwater arc discharge method and (b) current and voltage sensor setup.

The Elkahfi 100/ I-V Meter (Figure 2) is a versatile instrument that measures various electronic components' current-voltage (I-V) characteristics, such as solar cells, diodes, and sensors. Its current measurement range is 100 pA to 14 mA, and it can measure voltages up to 9.6 V with a 10-mV scanning step. This tool is commonly used in research and development to test the electrical characteristics of semiconductors and other materials. Its wide measurement range and advanced features make it an essential instrument for scientific and industrial applications requiring detailed current-voltage analysis.

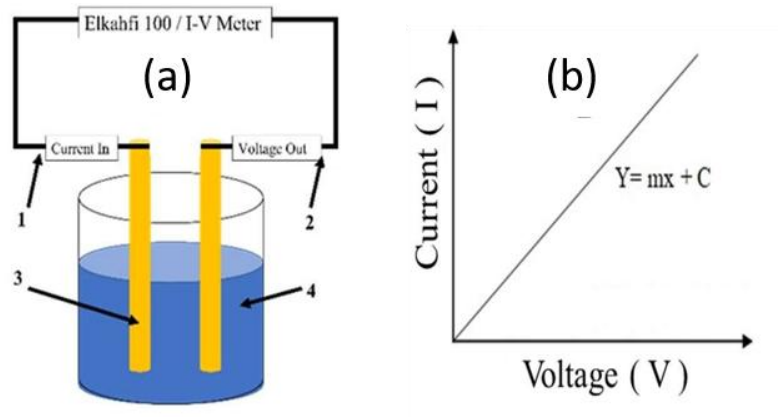

Figure 2. (a) Resistance testing schematic and (b) line gradient formula.

In our case, the Elkahfi 100/ I-V Meter was used to measure the resistance of produced nanoparticles, as shown in Figure 2. The measurement is done by adding 15 mg of nanoparticles into 5 ml of deionized water, which will then be measured with two probes connected to the Elkahfi 100/ I-V Meter. Figure 2(a) is a schematic image of resistance measurement using the Elkahfi 100/ I-V Meter, where numbered arrows are the input current probe (1), exit voltage probe (2), copper electrode (3), and solution medium (4) for testing nanoparticles, respectively. The resistance value [Figure 2(b)] can be determined using the line gradient formula equation as (1).

$$R = {}^{1}/_{m}\ (\Omega) \tag{1}$$

The electrical resistivity (ρ) can then be obtained as (2).

$$\rho = {}^{RA}/_{d}\ (\Omega\text{m}) \tag{2}$$

where R, d, and A are the resistance of the material (Ω), the distance between the two electrodes (m), and the electrode surface area (m^2), respectively.

3. RESULTS AND DISCUSSIONS

3.1. Current-Voltage Analysis of Arc Discharge

Figure 3 shows an arc discharge experiment of 40, 70, and 100 A arc current on an arc welding inverter. The graph shows that the arc does not appear immediately when the ignition starts. This is due to the movement of the anode and cathode slowly using the lever mounted on the tool, so that it takes time, and the distance between the electrodes is close enough that an arc will appear. The first peak plasma arc discharge current value experienced on-off conditions occurred 13 times, with the highest value at a current value of 152 A and the smallest at 114 A.

When the arc starts, the previously accumulated electrons on the anode begin to transfer to the cathode. Before this transfer, the accumulated electron charge at the anode creates a high potential difference between the anode and cathode. However, once the arc forms and the electron charge is redistributed, the potential difference between the anode and cathode decreases, which is reflected as a voltage reading. Further details regarding the generation of current and voltage can be found in [24].

The initial current (first peak) of the ON-state in Figure 3 indicates that the number of charges flowing between electrodes reached a maximum level due to the high capacitance value between the two electrodes. Thus, the value of the current first peak is relatively high for every applied current, as shown in Figure 4. After the first peak occurs, the current will stabilize at a certain value depending on the applied current. When the current value is increased, the arc current will also become larger following the current value of the source, i.e., 40 A [Figure 3(a)], 70 A [Figure 3(b)], and 100 A [Figure 3(c)]. The current oscillations in the arc current are the conditions when ionization of carbon electrodes takes place, which will produce carbon nanoparticles, as explained in detail in [22].

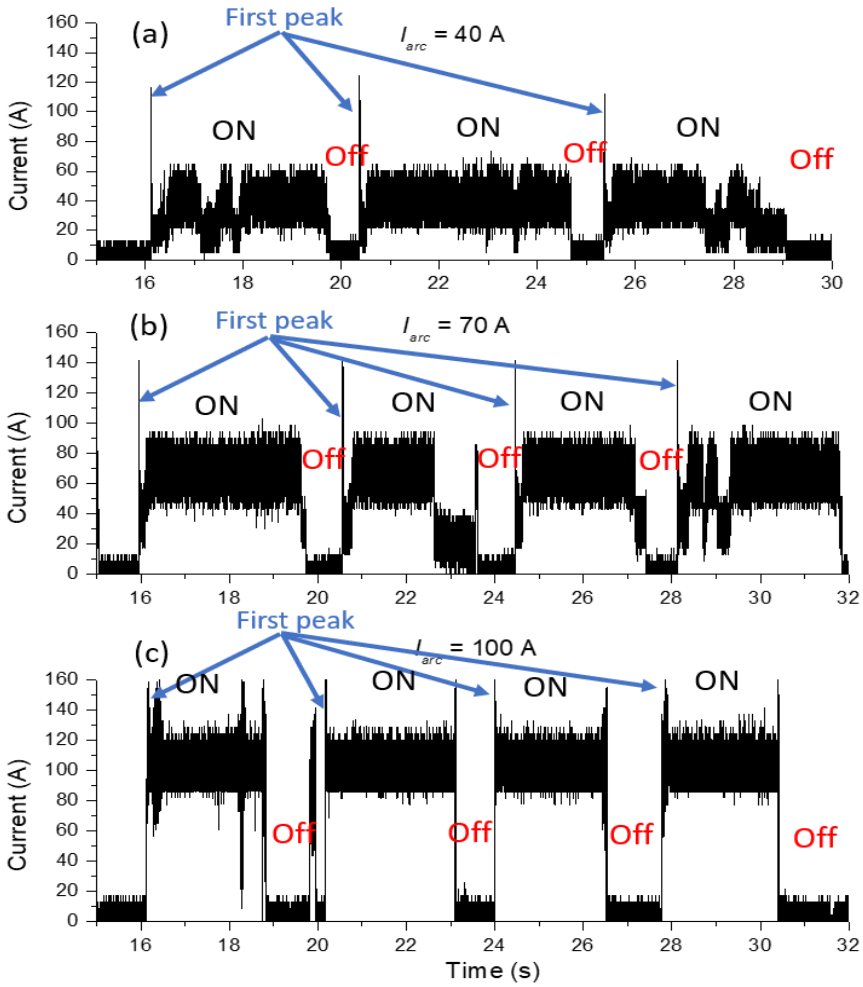

Figure 3. Arc current characteristics for (a) 40 A, (b) 70A and (c) 100 A. On-off states and first peaks clearly appear in the current graph.

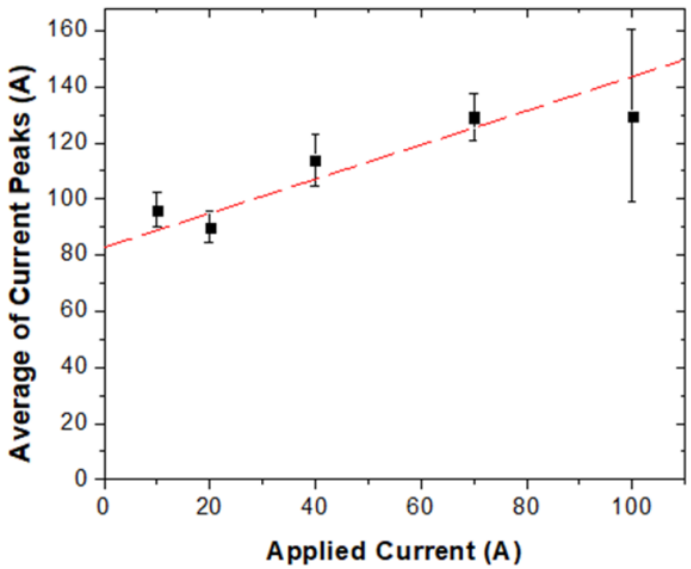

Figure 4. The average value of the first peak.

3.2. Carbon Nanoparticles Analysis

Figures 5(a-c) show the imaging results with high-resolution (HR) TEM images on samples with 40 A, 70 A, and 100 A arc currents. The nanoparticles' shape shows that the nanoparticles' characteristics are carbon nano-onion (CNO) and carbon nanotube (CNT) for all figures. However, Figures 5(b) and (c) also show other forms, including graphene carbon in sheet form and various amorphous structures. The inset of the images [Figure 5(a-c)] also shows a graph of the distribution of CNO and CNT length based on random samples. Based on the four graphs, the CNTs formed from the 40 A arc current have a more homogeneous size (around 150 nm length) than the other formation currents.

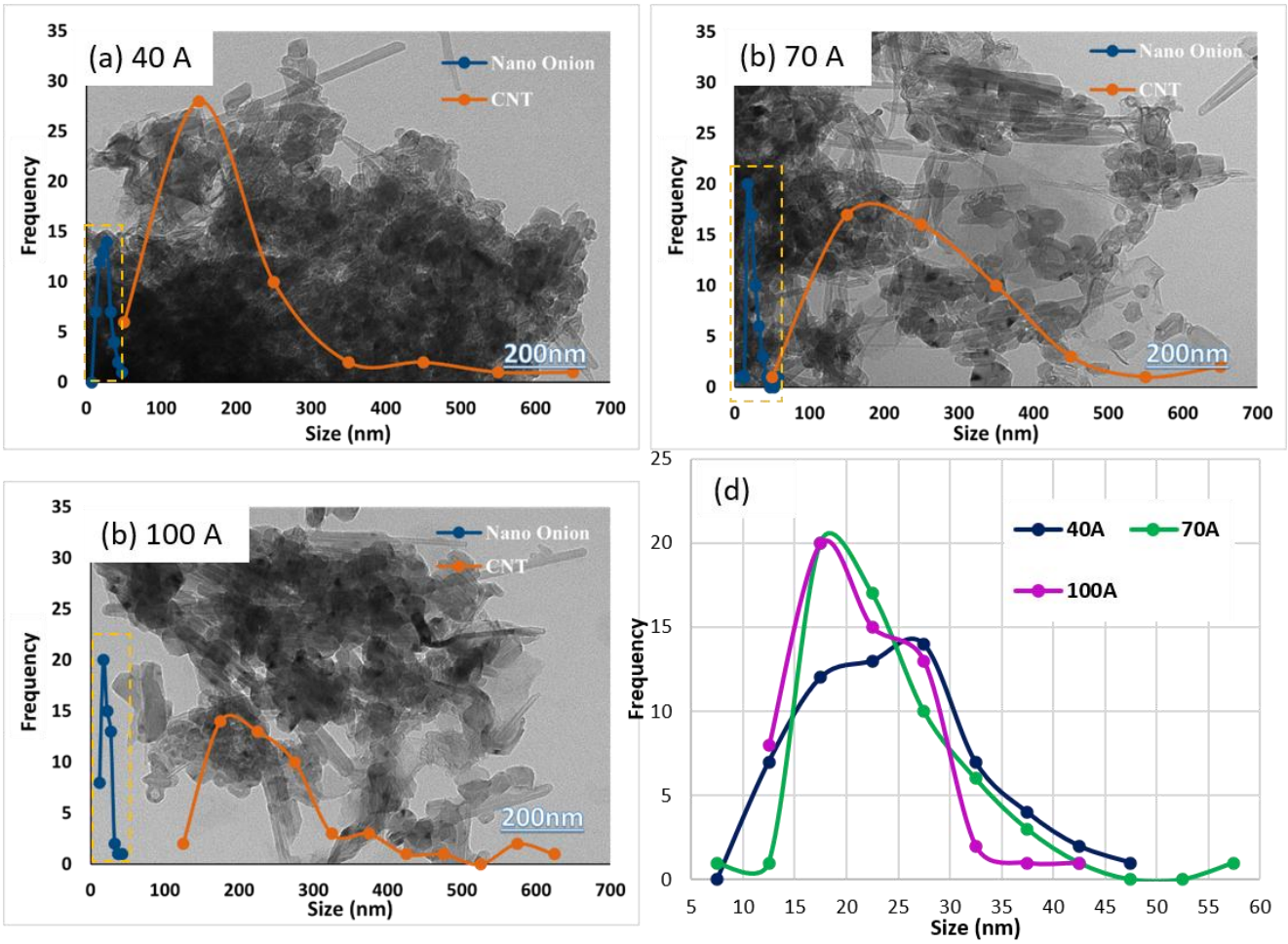

Figure 5. (a)-(c) TEM photograph of nanoparticle with size distribution graph in the inset. (d) zoom-in graph of carbon nano-onions distribution taken from inset graph (a)-(c) marked with a yellow dashed square.

Figure 5(d) is a magnification image of the nanoparticle distribution graph. Unlike the distribution of CNTs, which tends to vary, the size range of the CNO produced from the four experiments tends to be homogenous at 15 – 30 nm. Moreover, the shape of the CNOs in Figures 4(a-d) clearly show that a small CNT layer has formed.

I-V measurement using the Elkahfi 100/ I-V Meter produces a graph of current and voltage, as shown in Figure 6(a). The Elkahfi measurement result is then calculated into a resistance and resistivity value graph [Figure 6(b)] using equations (1) and (2), respectively, for different arc currents. The slope values, ranked from highest to lowest, are 40 A, 70 A, 100 A, and 10 A, as shown in Figure 6(a). Consequently, the resistivity of the nanoparticles corresponds to these slope values, with 40 A producing the lowest resistance compared to the others. This is most likely because the nanoparticles at 40 A are more homogeneous in shape [Figure 5(a)]. In contrast, the nanoparticles at 70 A and 100 A are less homogeneous and exhibit amorphous characteristics [see Figure 5(b)-(c)], resulting in higher resistance values.

Figure 7 shows an ionization energy distribution structure correlated with arc-generated carbon nanoparticles that, when the arc current is increased from 40 A to 100 A, transforms the product from predominantly carbon nano-onions to a high yield of carbon nanotubes (especially multi-walled CNTs). This coincides with dramatic changes in the in-situ ionization energy distribution derived from the arc I–V traces. At 40 A [see Figure 7(a)], the ionization energy distribution was essentially continuous from ~0 eV up to ~13 eV, indicating a broad spectrum of plasma species and collision energies. In this low-current regime, the arc plasma likely contains a mix of neutral carbon clusters, C^+ ions, and electrons with a wide Maxwellian-like energy spread. Such a continuous energy profile suggests that no single plasma process dominates; instead, carbon atoms

and clusters condense relatively randomly, consistent with the formation of quasi-spherical, closed-shell carbon nano-onions.

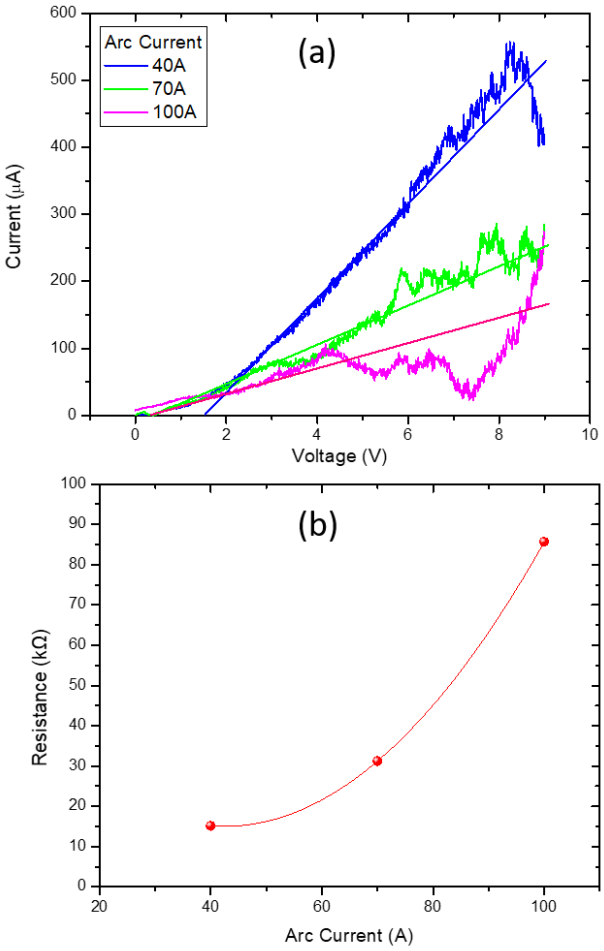

Figure 6. (a) I-V measurement results for three different arc currents and (b) resistance values taken from the slope of I-V data.

Indeed, prior studies have noted that arc discharges under milder conditions tend to produce fullerene-related structures: for example, the Sano group found that an arc in a rapidly quenching medium (liquid nitrogen) yielded mostly carbon onions [25], emphasizing how an environment favoring quick, equilibrium condensation encourages closed-shell morphology. In our case, the 40 A plasma's continuous energy spectrum implies a similar effect – carbon species cool and coalesce with minimal energetic bias, naturally forming multi-layered fullerene-like onions [see Figure 5(a)].

When the arc current is raised to 70 A, a clear transition in plasma kinetics occurs alongside the shift in morphology toward nanotubes. The ionization energy distribution becomes semi-discrete, developing distinct peaks at specific energies [Figure 7(b)]. Rather than a smooth continuum of energies, the 70 A plasma generates preferred ionization events at select energy values. This semi-discrete behavior suggests that specific ionization processes or plasma oscillations are now prevalent. A thermal distribution no longer dominates the plasma; instead, discrete packets of energy are delivered, possibly due to dynamic cathode spot activity or ion-acoustic wave structures in the arc column. This correlates with the appearance of tubular structures (CNTs) among the products [2] [see Figure 5(b)].

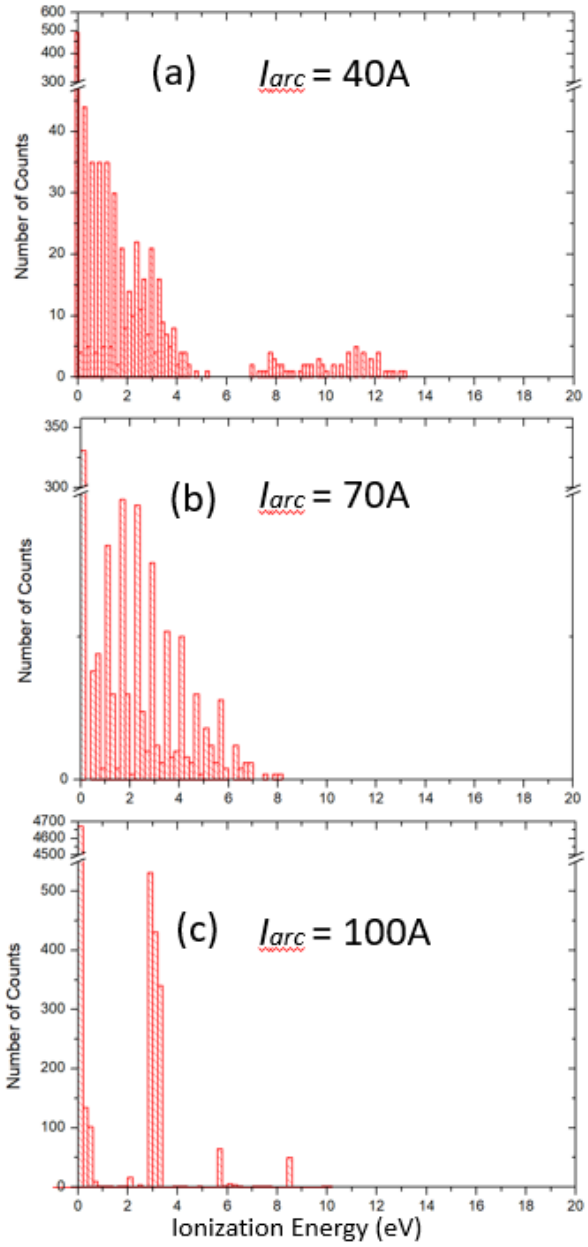

Figure 7. Ionization energy distribution of plasma arc discharge of (a) 40 A, (b) 70 A, and (c) 100 A arc current.

At the highest current of 100 A [Figure 7(c)], these trends intensify, yielding a plasma with highly discrete ionization energy behavior and a carbon product dominated by nanotubes. The ionization energy distribution at 100 A exhibits well-resolved peaks (e.g., around 0–1 eV, 2–4 eV, 5–6 eV, and 8–9 eV) with minimal continuum background. Such a discretized energy spectrum indicates that the arc discharge has entered a quantized energetic regime, where only specific ionization processes occur preferentially. This could arise from self-organized plasma oscillations or repetitive cathode spot eruptions delivering carbon in pulses of characteristic energy. In a high-current arc, the plasma is extremely ion-rich and dense; simulations of anodic arcs at similar currents have shown that ions can carry 70–90% of the total current [2], underscoring the strongly ionized nature of the 100 A discharge.

In other words, the 100 A arc is a highly organized plasma state compared to the 40 A and 70 A cases. Notably, experimental plasma studies have observed that as arc discharge current increases, the ion energy distribution can shift toward lower mean energies but with more intense, structured peaks [26]. This is consistent with our observations: the 100 A arc, despite its higher power, yields mostly low-to-moderate energy ions (sub-10 eV) grouped into peaks, rather than a broad high-energy spectrum. The higher plasma density at 100 A likely increases ion–ion and ion–neutral collisions, cooling many ions into the 0–6 eV range, while the strong electromagnetic forces in the arc organize the flow into energetic bursts, hence the multiple discrete peaks.

The emergence of highly discrete ionization behavior at 100 A is tightly linked to forming well-structured carbon nanotubes. Carbon nanotube growth in arc plasmas has long been attributed to the directed delivery of carbon in an ionized state [27]. Abramov et al. concluded that an arc plasma with a predominantly ionic composition can effectively transport carbon to the cathode and deposit it in an ordered manner, guided by electromagnetic forces [27].

In our high-current scenario, the strongly ionized carbon flux arrives at the cathode region where nanotubes grow, providing both the material feedstock and the kinetic energy to stimulate graphitic layer formation. The fact that nanotubes (cylindrical graphene layers) rather than onions (concentric graphitic shells) dominate at 100 A [see Figure 5(c)] suggests that open-ended growth has effectively won out over closed-shell growth. This aligns with the "graphene bubble" model proposed by Gupta [28].

4. CONCLUSION

The results of this study demonstrate a strong interdependence between arc current, plasma ionization characteristics, nanoparticle morphology, and the electrical behavior of carbon nanostructures synthesized via submerged arc discharge. The plasma maintains a continuous ionization energy distribution at lower arc current (40 A), forming predominantly isotropic, spherical carbon nano-onions. These particles exhibit relatively low electrical resistance due to their larger size and partial graphitic connectivity. As the arc current increases to 70 A and 100 A, the plasma becomes increasingly ionized, and the ionization energy distribution transitions to discrete peaks, indicating organized energy transfer mechanisms within the arc. These discrete plasma states favor the anisotropic growth of carbon nanostructures, resulting in a shift toward multi-walled carbon nanotubes at higher currents. Simultaneously, the measured electrical resistance increases significantly, which is attributed to the decrease in conductive pathway connectivity among the more fragmented and agglomerated particles at higher arc energies.

These findings collectively suggest that the arc current not only governs plasma energetics and nanoparticle nucleation but also critically shapes the final morphology and electrical properties of the carbon materials. By tuning arc parameters, particularly discharge current, one can strategically steer nanoparticle formation toward desired structural and functional outcomes, making this process a promising tool for scalable synthesis of application-specific carbon nanomaterials.

ACKNOWLEDGMENTS

We thank A.C. Putri for her support in the experiment and discussion. This work was partially supported by Grants-in-Aid for Prototype (No: 023.1/UN27.22/PT.01.03/2024) from Ministry of Higher Education, Research and Technology and Grants-in-Aid for Fundamental Research (No: 228/UN27.22/PT.01.03/2023 and Grants-in-Aid for Research Group (no: 371/UN27.22/PT.01.03/2025) from Sebelas Maret University.

AUTHOR CONTRIBUTIONS

All authors contributed to analyzing the results and reviewing the manuscript.

CONFLICTS OF INTEREST

The manuscript has not been published elsewhere and is not being considered by other journals. All authors have approved the review, agreed with its submission, and declared no conflict of interest regarding the manuscript.

REFERENCES

[1] G. A. Mansoori and T. A. Fauzi Soelaiman, "Nanotechnology — An Introduction for the Standards Community," *Journal of ASTM International,* vol. 2, no. 6, p. JAI13110, 2005, doi: 10.1520/JAI13110.

[2] M. Keidar, et al.,, ""Mechanism of carbon nanostructure synthesis in arc plasma",," *Physics of Plasmas,* vol. 17, no. 5, p. 057101, 2010.

[3] B. Sundqvist, "Carbon under pressure," *Physics Reports,,* vol. 909, pp. 1-73, 2021.

[4] A. Bianco, et al.,, "Carbon science perspective in 2020: Current research and future challenges," *Carbon,* vol. 161, pp. 373-391, 2020.

[5] B. Vedhanarayanan, et al., "Hybrid materials of 1D and 2D carbon allotropes and synthetic π-systems," *NPG Asia Materials,* vol. 10, no. 4, pp. 107-126, 2018.

[6] J. Pang *et al.*, "CVD growth of 1D and 2D sp 2 carbon nanomaterials," *Journal of materials science,* vol. 51, pp. 640-667, 2016.

[7] A. K. Geim, and K.S. Novoselov, "The rise of graphene," *Nature Materials,* vol. 6, no. 3, pp. 183-191, 2007.

[8] H. W. Kroto, et al., "C60: Buckminsterfullerene," *Nature,* vol. 318, no. 6042, pp. 162-163, 1985.

[9] R. E. Smalley, "Great balls of carbon: The story of buckminsterfullerene," *The Sciences,* vol. 31, no. 2, pp. 22-28, 1991.

[10] S. Iijima, "Carbon nanotubes: past, present, and future," *Physica B: Condensed Matter,* vol. 323, no. 1-4, pp. 1-5, 2002.

[11] S. Iijima, "Helical microtubules of graphitic carbon," *Nature,* vol. 354, no. 6348, pp. 56-58, 1991.

[12] S. Jafari, *Carbon Nanotube-Reinforced Polymers*. Cambridge: Elsevier, 2018.

[13] S. K. Soni, B. Thomas, and V.R. Kar, "A comprehensive review on CNTs and CNT-reinforced composites: syntheses, characteristics and applications," *Materials Today Communications,* vol. 25, p. 101546, 2020.

[14] Y. Li, "Carbon nanotube research in its 30th year. 2021," *ACS Nano,* vol. 15, no. 6, pp. 9197-9200, 2021.

[15] M. Zheng, et al., "Carbon nanotube-based materials for lithium–sulfur batteries," *Journal of Materials Chemistry A,* vol. 7, no. 29, pp. pp. 17204- 17241, 2019.

[16] A. H. Sari, A. Khazali and S.S. Parhizgar, "Synthesis and characterization of long-CNTs by electrical arc discharge in deionized water and NaCl solution," *International Nano Letters,* vol. 8, no. 1, pp. 19- 23, 2018.

[17] S. Rathinavel, K. Priyadharshini, and D. Panda, "A review on carbon nanotube: An overview of synthesis, properties, functionalization, characterization, and the application," *Materials Science and Engineering: B,* vol. 268, p. 115095, 2021.

[18] N. Gupta, S.M. Gupta and S. Sharma, "Carbon nanotubes: Synthesis, properties and engineering applications," *Carbon Letters,* vol. 29, no. 5, pp. 419-447, 2019.

[19] N. Sano *et al.*, "Properties of carbon onions produced by an arc discharge in water," *Journal of Applied Physics,* vol. 92, no. 5, pp. 2783-2788, 2002.

[20] F. Alessandro, et al., "Selective synthesis of turbostratic polyhedral carbon nano-onions by arc discharge in water," *Nanotechnology,* vol. 29, no. 32, p. 325601, 2018.

[21] M. Anwar, T. E. Saraswati and A. Bahrudin, "Submerged electrical arc discharge for nanoparticles fabrication using carbon-based electrodes," *Materials Science Forum,* vol. 939, pp. 141-146, 2018.

[22] M. Anwar, et al., "Probing ionization characteristics of under-water plasma arc discharge using simultaneous current and voltage versus time measurement in carbon nanoparticle synthesis," *Micro and Nano Engineering,* vol. 14, p. 100099, 2022.

[23] M. Anwar, R. R. Kusuma, and T. E. Saraswati, "Critical Role of Carbon Electrode Properties in Submerged Arc Plasma Behavior and Resulting Nanocarbon Particle Morphology," *IEEE Transactions on Plasma Science,* pp. 1-10, 2025, doi: 10.1109/TPS.2025.3630183.

[24] A. C. Putri, anwar, M., et al., "Plasma Characteristics of Under-water Arc Discharge in Nanoparticle Fabrication," *Journal of Electrical, Electronic, Information, and Communication Technology,* vol. vol. 4, no. 1, pp. 11- 15, 2022.

[25] I. Alexandrou, H. Wang, N. Sano, and G. A. J. Amaratunga, "Structure of carbon onions and nanotubes formed by arc in liquids," *The Journal of Chemical Physics,* vol. 120, no. 2, pp. 1055-1058, 2004, doi: 10.1063/1.1629274.

[26] A. Borisenko, "Dynamics of the ion energy distribution and plasma parameters in flows of the non-self-sustained arc discharge in molybdenum vapors," *Problems of Atomic Science and Technology,* vol. 29, p. 4, 2023.

[27] G. Abramov, A. Ivanov, and G. Popov, "Hydrodynamic description of the mechanism of formation of carbon nanotubes," *Journal of Engineering Physics and Thermophysics,* vol. 80, no. 6, pp. 1116-1123, 2007.

[28] V. Gupta, "Graphene as intermediate phase in fullerene and carbon nanotube growth: A Young–Laplace surface-tension model," *Applied Physics Letters,* vol. 97, no. 18, 2010.

[29] E. Moreau and E. Defoort, "Effect of the high voltage waveform on the ionic wind produced by a needle-to-plate dielectric barrier discharge," *Scientific Reports,* vol. 12, no. 1, p. 18699, 2022.

[30] C. Tauber *et al.*, "Characterization of a non-thermal plasma source for use as a mass specrometric calibration tool and non-radioactive aerosol charger," *Atmospheric Measurement Techniques,* vol. 13, no. 11, pp. 5993-6006, 2020.

[31] F. J. Chao-Mujica *et al.*, "Carbon quantum dots by submerged arc discharge in water: Synthesis, characterization, and mechanism of formation," *Journal of Applied Physics,* vol. 129, no. 16, 2021, doi: 10.1063/5.0040322.